Estimating Gale to Hurricane Force Winds Using the Satellite Altimeter

YVES QUILFEN

Space Oceanography Laboratory, IFREMER, Plouzané, France

DOUG VANDEMARK

Ocean Process Analysis Laboratory, University of New Hampshire, Durham, New Hampshire

BERTRAND CHAPRON

Space Oceanography Laboratory, IFREMER, Plouzané, France

HUI FENG

Ocean Process Analysis Laboratory, University of New Hampshire, Durham, New Hampshire

JOE SIENKIEWICZ

Ocean Prediction Center, NCEP/NOAA, Camp Springs, Maryland

(Manuscript received 21 September 2010, in final form 29 November 2010)

ABSTRACT

A new model is provided for estimating maritime near-surface wind speeds (U_{10}) from satellite altimeter backscatter data during high wind conditions. The model is built using coincident satellite scatterometer and altimeter observations obtained from QuikSCAT and Jason satellite orbit crossovers in 2008 and 2009. The new wind measurements are linear with inverse radar backscatter levels, a result close to the earlier altimeter high wind speed model of Young (1993). By design, the model only applies for wind speeds above 18 m s^{-1}. Above this level, standard altimeter wind speed algorithms are not reliable and typically underestimate the true value. Simple rules for applying the new model to the present-day suite of satellite altimeters (*Jason-1*, *Jason-2*, and *Envisat* RA-2) are provided, with a key objective being provision of enhanced data for near-real-time forecast and warning applications surrounding gale to hurricane force wind events. Model limitations and strengths are discussed and highlight the valuable 5-km spatial resolution sea state and wind speed altimeter information that can complement other data sources included in forecast guidance and air–sea interaction studies.

1. Introduction

It is widely recognized that satellite radar altimeters can accurately measure ocean wind speed from 0 to 20 m s^{-1} (Witter and Chelton 1991; Gourrion et al. 2002; Zieger et al. 2009), but limited attention has been given to the generation or validation of altimeter products for wind speeds above 15–18 m s^{-1} where buoy measurements, the standard ground truth, become sparse. Young (1993), followed by Quilfen et al. (2006, 2010), shows that the same physical and empirical inverse relationship between surface roughness and altimeter signal backscatter applies at high winds, at least up to speeds of 35 m s^{-1}, and several reasons to renew focus on high winds from altimetry now exist. These include the present and future likelihood that several satellite altimeters will be in orbit at any given time and, as now, they can provide desirable near-real-time data to meteorological centers. Next, although the altimeter coverage is very limited because of its narrow swath, accurate wind speed plus sea state data at 5–10-km resolution within intense small-scale tropical and extratropical cyclone events is clearly very useful and unique for forecasts, hindcasts (Cardone et al. 2009), and offshore design applications

Corresponding author address: Yves Quilfen, IFREMER, Centre de Brest, BP70, 29280 Plouzané, France.
E-mail: yves.quilfen@ifremer.fr

DOI: 10.1175/JTECH-D-10-05000.1

(Caires and Sterl 2005) when it can be gained. Finally, some advancement has come in our ability to gain calibration data for high-speed altimeter model development since the innovative study of Young (1993), where six passes of *Geosat* altimeter data were coregistered with winds predicted from a tropical cyclone model.

This article follows on from Young (1993) to develop a simple Ku-band radar model for improved altimeter wind speeds at high winds (above 18 m s^{-1}). The approach makes use of high wind speed event data collected where altimeter (from *Jason-2*) and wind vector scatterometer (QuikSCAT) ground tracks coincide. In contrast to the altimeter, much focus has been given to refinement and validation of high wind speed measurements from this scatterometer (e.g., Schulz et al. 2007; Yuan 2004; Sampe and Xie 2007) to show its ability to accurately (~2 m s^{-1} root-mean-square error) measure events not resolved in global weather prediction products.

The resulting model should apply for any upcoming or past altimeter as long as Ku-band backscatter data are properly intercalibrated using an offset scalar. We include some demonstration of the results that should be gained using the present-day *Jason-2* system. While a more in-depth use of satellite radar and radiometer data for high wind measurements can be devised for precision altimeter platforms (e.g., *Jason-2*) where multiple frequency observations are available (cf. Quilfen et al. 2010), this study focuses on a monofrequency Ku-band radar backscatter model that is easily created and handled across multiple platforms.

2. Datasets

Much attention has recently been given to improving satellite scatterometer ocean wind estimates at levels above 15 m s^{-1} (Fernandez et al. 2006; Yueh et al. 2001), leading to the revised QuikSCAT high wind model function QSCAT-1/F13 (Callahan 2006). Given that these QuikSCAT observations were in use at the National Centers for Environmental Prediction (NCEP) for storm forecasting and guidance purposes up to the final satellite data in November 2009, we choose to use QuikSCAT to develop an altimeter model that will yield a similar behavior. We have produced a match up of *Jason-2* altimeter Ku-band normalized radar backscatter and QuikSCAT scatterometer wind speed over a period extending from July 2008 to November 2009. The time limit between satellite observations must be less than 1 h and the spatial distance less than 25 km. Altimeter data come from the *Jason-2* Geophysical Data Records (GDR) version C (Dumont et al. 2009), and QuikSCAT data are level 2B products, from version 2.4 implemented in 2006 (Callahan 2006). Data have been edited to eliminate measurements contaminated by rain by the standard QuikSCAT and/or *Jason-2* rain flags and by radiometer liquid water content exceeding 0.2 kg m^{-2}. That resulting QuikSCAT/*Jason-2* subset contains 3177 data points having QuikSCAT wind speeds between 18 and 30 m s^{-1}. For model validation we will include use of a separate but similar (same time period, same editing criteria) crossover dataset between the *Jason-1* altimeter and QuikSCAT. This validation dataset contains 3002 data points.

3. The high wind model and its validation

a. A new high wind altimeter model consistent with QuikSCAT

The upper panel of Fig. 1 shows the *Jason-2* Ku-band normalized radar cross section (NRCS) as a function of the altimeter's GDR product wind speed for the complete 2008–09 dataset. Results reflect typical altimeter wind algorithm behavior [for a recent review, see Fig. 5 in Zieger et al. (2009)]. The GDR algorithm, used to compute the *Jason-1* and *-2* GDR winds, follows from Gourrion et al. (2002) and is a two-parameter function that primarily relates wind speed to NRCS, but it also includes the second-order impact from significant wave height (SWH). The GDR algorithm was calibrated by comparing *Jason-1* NRCS to QuikSCAT scatterometer wind speed data derived from a geophysical model function (GMF) defined at the early stage of the QuikSCAT mission. This GMF was known to underestimate the high wind speed (Fernandez et al. 2006). This partly explains the altimeter wind speed saturation as observed in the upper panel of Fig. 1, with no altimeter wind values higher than gale wind category (~24 m s^{-1}). Another contributor to high wind error in this GDR algorithm is the paucity of high wind data that were available to train the algorithm.

The lower panel in Fig. 1 shows *Jason-2* NRCS as a function of coregistered QuikSCAT wind speed data. A well-defined altimeter NRCS decrease with increasing QuikSCAT wind speed is observed up to hurricane force winds, but matchup data are lacking above this level. The dashed curve in Fig. 1 represents the Young (1993) model. It is clear this linear *Geosat* model lies near the data but slightly underestimates the NRCS saturation at highest winds.

The proposed new high-wind altimeter model function branch, also shown in Fig. 1, is again a linear model relating NRCS to 10-m wind speeds above 18 m s^{-1}. As seen in the upper panel of Fig. 1, the second-order SWH contribution to the GDR wind model (i.e., the wind speed scatter at constant NRCS) vanishes with increasing wind speed (Gourrion et al. 2002). Thus we can expect an accurate transition to an NRCS-only high wind algorithm beyond 18 m s^{-1}.

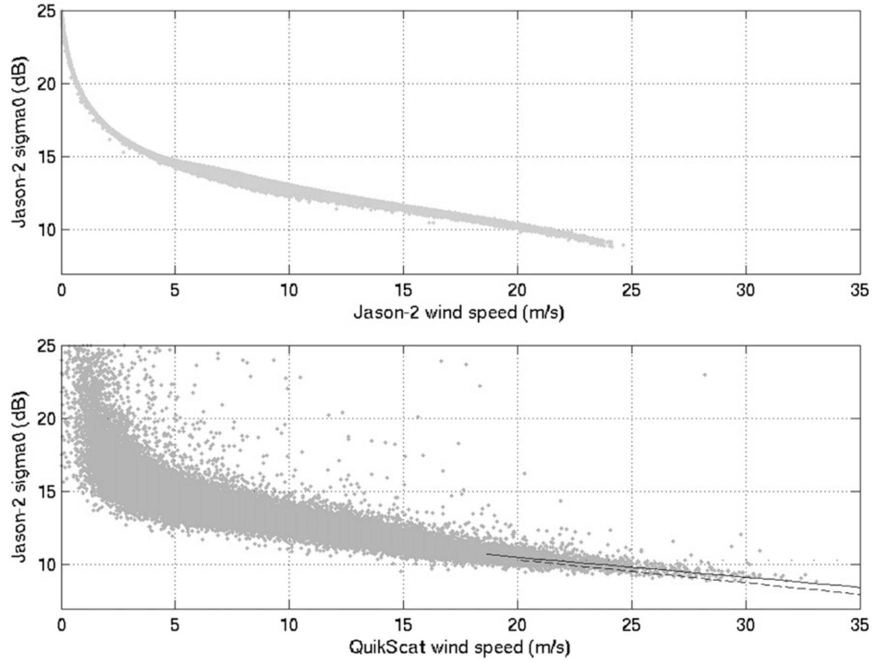

FIG. 1. Behavior of *Jason-2* Ku-band altimeter NRCS (dB) as a function of the (top) *Jason-2* and (bottom) QuikSCAT wind speed (m s^{-1}). The new (solid) and Young (dashed) high wind models are shown.

The new model coefficients were derived using an orthogonal regression between the QuikSCAT and *Jason-2* data for wind speeds between 18 and 30 m s^{-1} to obtain

$$U_{10} = 96.98 - 7.32(\mathrm{NRCS} + \mathrm{offset}) \quad \text{for} \quad \mathrm{NRCS} < 10.7896\,\mathrm{dB}, \tag{1}$$

where the Ku-band NRCS has units of decibels (dB) and U_{10} is the 10-m wind speed in units of meters per second. The variable ''offset'' is an adjustment needed to apply the linear model to altimeters other than *Jason-2* and simply adjusts the absolute value of the backscatter for intersensor calibration differences. For example, the offset with *Jason-2* for the *Jason-1* and *Envisat* RA-2 altimeters now in orbit are 0.0 and 2.8 dB, respectively (Queffelou and Croizé-Fillon 2010). At this time we assume there is no time drift in the NRCS observations but this possibility will need to be monitored. The choice to use the NRCS threshold value rather than an altimeter wind speed was found to provide a more robust fit and continuous transition between GDR model and QuikSCAT data near 18 m s^{-1} wind speed.

Figure 1 shows that the new model gives a slightly greater NRCS wind sensitivity than the Young algorithm, consistent with a possible wind speed underestimation of that model as discussed in Quilfen et al. (2010). To illustrate the difference between the two algorithms, a 9-dB NRCS yields a wind speed of 31.1 m s^{-1} for the new algorithm and 28.5 m s^{-1} for Young (1993), an 8% difference.

b. Validation

Figure 2 shows results for altimeter versus scatterometer wind using the altimeter standard GDR model (top left) and then, at high wind (bottom), the new model. This is shown separately for the *Jason-1* and *Jason-2* colocation datasets as described in the data section, the former being independent from the data used to develop Eq. (1). The spread of data density contours on the bottom panels is indicative of similar wind speed distributions for both systems. An orthogonal regression between the altimeter and the scatterometer winds across all speeds (Fig. 2, upper right) gives 1.016 (0.993) for the slope, −0.11 (−0.4) for the intercept, and 1.04 (1.02 m s^{-1}) for the root-mean-square error for *Jason-2* (*Jason-1*). The rms differences observed for *Jason-2* and the independent *Jason-1* datasets are quite similar and the levels are of the order of altimeter wind model agreement with buoys seen at moderate winds (i.e., lower than 1.5 m s^{-1}) (e.g., Gourrion et al. 2002; Zieger et al. 2009). When limiting to winds beyond 18 m s^{-1}, it gives 1.017 (0.999), −0.08 (0.07), and 1.81 (1.85 m s^{-1}), which gives rms differences lower than the usual prelaunch specifications for the wind sensors (~2 m s^{-1}). This agreement and comparison against an independent dataset lead us to assume the new model

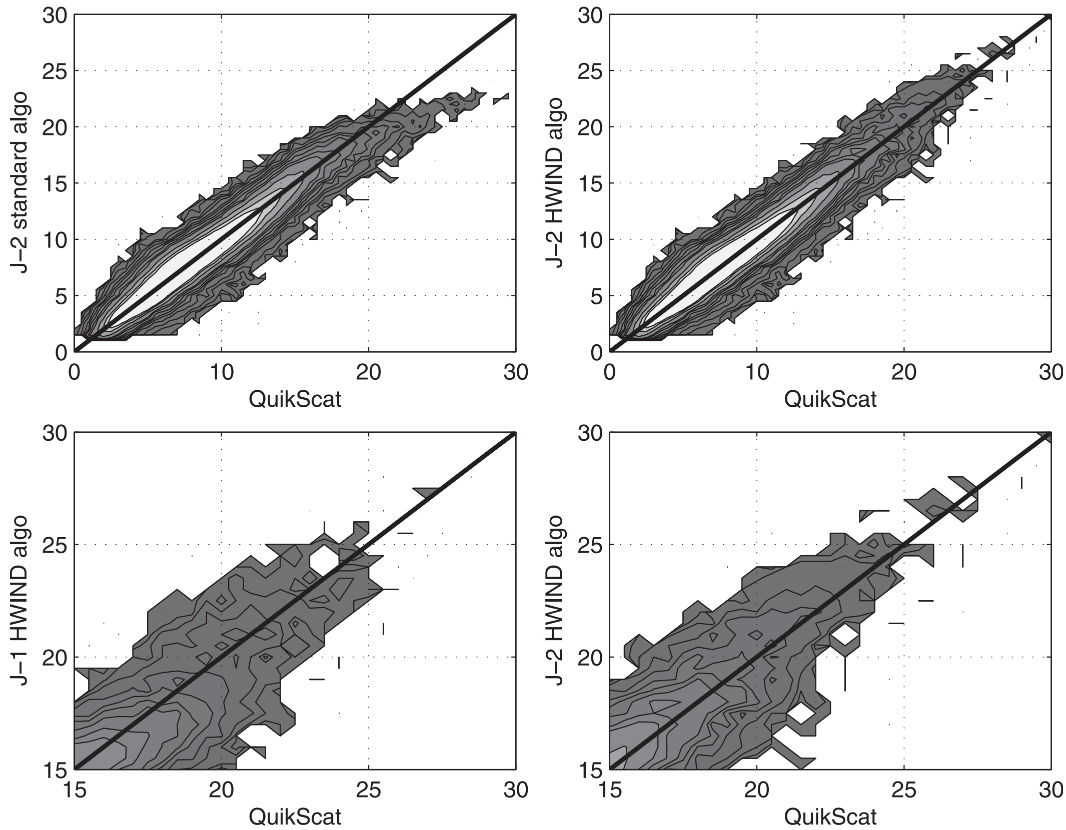

FIG. 2. Scatterplots of the altimeter-retrieved wind speed (m s^{-1}) as a function of the QuikSCAT wind speed (m s^{-1}). (top left) *Jason-2* standard wind speed; (top right) *Jason-2* with the high wind branch included; (bottom right) focus on new *Jason-2* high wind model branch; (bottom left) focus on *Jason-1* with the new high wind branch. Contours represent the data density.

represents a QuikSCAT-consistent high wind speed altimeter result.

4. Data demonstrations using the revised altimeter winds

Further model validation beyond our use of QuikSCAT is difficult, as is validation of any high wind sensor at sea. For winds above 20 m s^{-1}, the buoy measurements often used as reference are rare and are likely to underestimate winds because of large hull movements and shadowing by waves. As one approach to further validation, we choose to illustrate the sensitivity of the altimeter and scatterometer measurements to hurricane force winds as well as their coherency with SWH measured by the altimeter. Two separate storm systems are observed in Fig. 3, one (right) in the Indian Ocean (7 October 2008; QuikSCAT orbit 48442; *Jason-2* cycle 9 orbit 203) and the other (left) in the Atlantic Ocean (16 January 2009; QuikSCAT orbit 49881; *Jason-2* cycle 19 orbit 250) . These chosen cases are rain-free for the most part. Data show the QuikSCAT wind speed (25-km resolution), the altimeter track (solid line), and the storm track every 6 h (dotted line). The QuikSCAT wind field shown on Fig. 3 has been translated in space to be valid at the *Jason-2* pass time. The time difference between the QuikSCAT and *Jason-2* measurements is 4 h 53 min (2 h) for the Indian (Atlantic) Ocean storm. As shown, the Indian Ocean storm is fast moving, while the Atlantic system is almost stationary for the days nearest to the altimeter storm visit time. The wind strength and durations thus lead to substantially different fetch conditions for the sea state development.

Interpolation of observations to a common time/space reference allows the nearly direct wind speed comparison (see also Fig. 4) shown in Fig. 3. The evaluation is imposed at the altimeter track locations, and the comparison accounts for the time difference between *Jason-2* and QuikSCAT times by using a storm-centric coordinate system that uses the storm speed to translate the QuikSCAT wind field to the altimeter track. The *Jason-2* and QuikSCAT wind segments are in good agreement

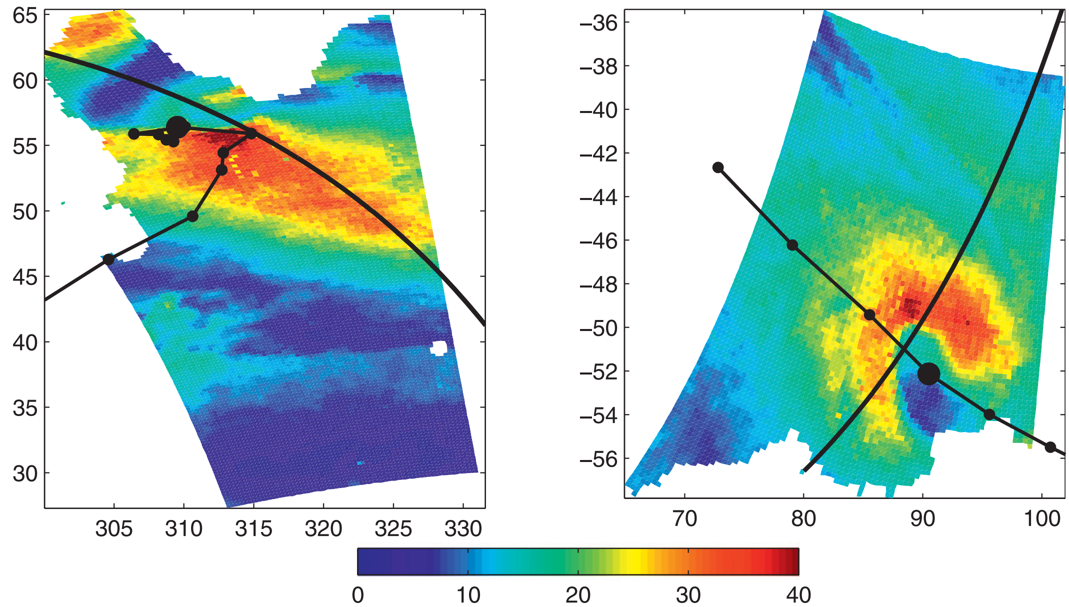

FIG. 3. The QuikSCAT wind speed field (m s^{-1}), *Jason-2* sampling track (solid line), and 6-hourly storm center location estimates (black circles) for the (left) North Atlantic and (right) southern Indian Ocean storm events. The larger dot indicates the 6-h synoptic storm location closest to the *Jason-2* time. Storm center location is estimated by finding the maximum relative vorticity in the storm from the 6-hourly Japanese 25-yr Reanalysis (JRA-25) numerical atmospheric reanalysis vorticity fields.

although the different measurement times (~2 h and 4 h 50 min for the Atlantic and South Indian storms, respectively) likely induce some difference. The moderate rain rate may also impact the QuikSCAT-retrieved wind speed. Typically rain reduces the QuikSCAT retrieved wind speed by about 5 m s^{-1} at 10 mm h^{-1} and 30 m s^{-1} (Tournadre and Quilfen 2003). This is the case for the Atlantic storm between 315° and 316° longitude where the QuikSCAT wind speed is lower. Indeed, both the *Jason-2* and QuikSCAT radiometers indicate significant liquid water content, although the QuikSCAT rain flag is not set as often at high wind speed.

Very large wind speed gradients are retrieved from the higher-resolution altimeter measurements for the Atlantic storm (Fig. 4, top). Using the 12.5-km resolution QuikSCAT data does not bring additional information, and it results in a much noisier wind speed field. A remarkable result is the agreement between the maximum wind speed measured by the two sensors in both storms, giving good confidence in the satellite-observed cross storm asymmetries and gale/storm wind radii. For the Atlantic storm, winds close to hurricane force extend for hundreds of kilometers beyond the sharp front, where they cover a much smaller area for the South Indian storm.

The corresponding and coincident altimeter SWH data are certainly to be exploited to improve storm characterization. For the Indian Ocean storm, *Jason-2* intersected the hurricane-force wind region and measured SWH locally of the order of 12 m. The northern Atlantic storm was almost steady for 2 days near the *Jason-2* overflight and this exceptionally long fetch results in a wide ocean area of extreme sea conditions (SWH > 15 m). Although maximum observed winds are higher for the Indian Ocean storm, the maximum significant wave height is lower because of the shorter duration conditions.

5. Summary

This article revisits and reaffirms the fact that ocean satellite altimetry can retrieve wind speeds from the radar backscatter in gale to storm conditions as shown in Young (1993). The newly proposed high wind altimeter wind model is a simple training of the altimeter to data from the latest scatterometer (QuikSCAT) high wind product and thus it should yield data that are consistent with satellite products that forecast offices now consider valuable and operational. Extracting viable altimeter data at higher wind speeds than the standard science team products should now enable us to obtain coherent wind and sea state information in extreme seas. Such dual measurements, although narrow swath, represent a strong complement to other satellite wind imagers in near-real-time applications.

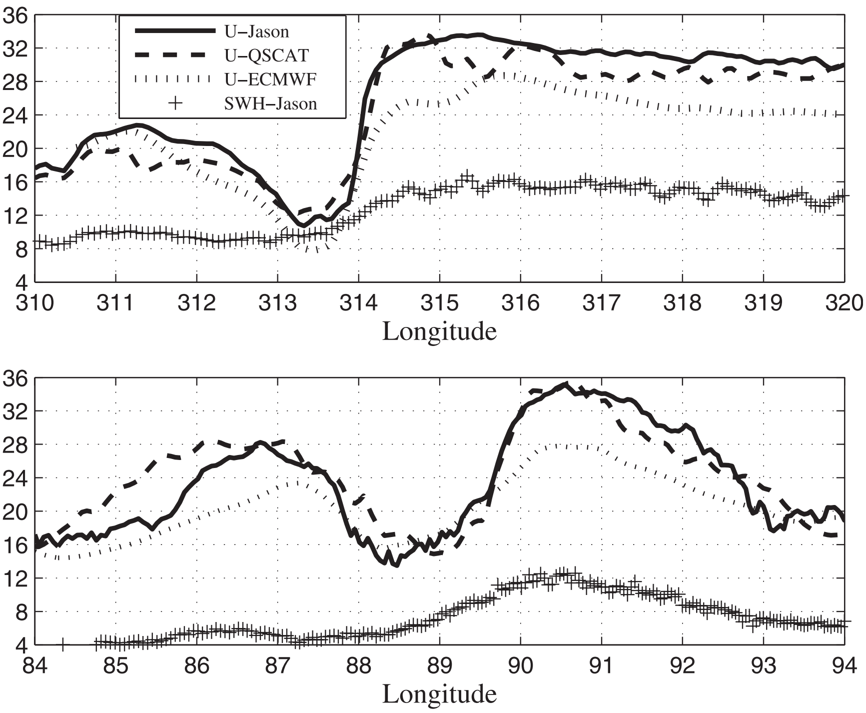

FIG. 4. Collocated U_{10} wind speed (m s^{-1}) profiles along the altimeter track: *Jason-2* (solid), QuikSCAT (dashed), and ECMWF at 0.25° resolution (dotted) for the (top) North Atlantic and (bottom) southern Indian Ocean storms. *Jason-2* significant wave height measurements (m) are also shown.

REFERENCES

Caires, S., and A. Sterl, 2005: 100-year return value estimates for ocean wind speed and significant wave height from the ERA-40 data. *J. Climate,* **18,** 1032–1048.

Callahan, P. S., 2006: QuikSCAT science data product user's manual: Overview and geophysical data products, version 3.0. JPL Rep. D-18053-RevA, 85 pp. [Available online at ftp://podaac.jpl.nasa.gov/pub/ocean_wind/quikscat/doc/QSUG_v3.pdf.]

Cardone, V. J., A. T. Cox, M. A. Morrone, and V. R. Swail, 2009: Satellite altimeter detection of global very extreme sea states (VESS). *Proc. 11th Int. Workshop on Wave Hindcasting and Forecasting,* Halifax, Canada, JCOMM. [Available online at http://www.waveworkshop.org/11thWaves/.]

Dumont, J. P., and Coauthors, 2009: OSTM/*Jason-2* products handbook. CNES Rep. SALP-MU-M-OP-15815-CN, ed. 1.4, 67 pp. [Available online at http://www.osdpd.noaa.gov/ml/ocean/J2_handbook_v1-4_no_rev.pdf.]

Fernandez, D. E., J. R. Carswell, S. Frasier, P. S. Chang, P. G. Black, and F. D. Marks, 2006: Dual-polarized C- and Ku-band ocean backscatter response to hurricane-force winds. *J. Geophys. Res.,* **111,** C08013, doi:10.1029/2005JC003048.

Gourrion, J., D. Vandemark, S. Bailey, B. Chapron, C. P. Gommenginger, P. G. Challenor, and M. A. Srokosz, 2002: A two-parameter wind speed algorithm for Ku-band altimeters. *J. Atmos. Oceanic Technol.,* **19,** 2030–2048.

Queffeulou, P., and D. Croizé-Fillon, 2010: Global altimeter SWH data set, version 7. Ifremer. [Available online at ftp://ftp.ifremer.fr/ifremer/cersat/products/swath/altimeters/waves/documentation/altimeter_wave_merge__7.0.pdf.]

Quilfen, Y., B. Chapron, and J. Tournadre, 2006: Altimeter dual-frequency observations of surface winds, waves, and rain rate in tropical cyclone Isabel. *J. Geophys. Res.,* **111,** C01004, doi:10.1029/2005JC003068.

——, ——, and ——, 2010: Satellite microwave surface observations in tropical cyclones. *Mon. Wea. Rev.,* **138,** 421–437.

Sampe, T., and S.-P. Xie, 2007: Mapping high sea winds from space: A global climatology. *Bull. Amer. Meteor. Soc.,* **88,** 1965–1978.

Schulz, E. W., J. D. Kepert, and D. J. M. Greenslade, 2007: An assessment of marine surface winds from the Australian Bureau of Meteorology numerical weather prediction systems. *Wea. Forecasting,* **22,** 613–636.

Tournadre, J., and Y. Quilfen, 2003: Impact of rain cell on scatterometer data: 1. Theory and modeling. *J. Geophys. Res.,* **108,** 3225, doi:10.1029/2002JC001428.

Witter, D. L., and D. B. Chelton, 1991: A Geosat altimeter wind speed algorithm and a method for wind speed algorithm development. *J. Geophys. Res.,* **96,** 8853–8860.

Young, I. R., 1993: An estimate of the Geosat altimeter wind speed algorithm at high wind speeds. *J. Geophys. Res.,* **98,** 20 275–20 285.

Yuan, X. J., 2004: High-wind-speed evaluation in the Southern Ocean. *J. Geophys. Res.,* **109,** D13101, doi:10.1029/2003JD004179.

Yueh, S. H., B. W. Stiles, W. Y. Tsai, H. Hu, and T. W. Liu, 2001: QuikSCAT geophysical model function for tropical cyclones and application to Hurricane Floyd. *IEEE Trans. Geosci. Remote Sens.,* **39,** 2601–2612, doi:10.1109/36.974995.

Zieger, S., J. Vinoth, and I. R. Young, 2009: Joint calibration of multiplatform altimeter measurements of wind speed and wave height over the past 20 years. *J. Atmos. Oceanic Technol.,* **26,** 2549–2564.